

ing no antibodies. Transcription reactions for U6 and Ad2 ML were carried out as described by Lobo *et al.* (7). Purified GST-hTBP proteins were added as indicated in the figure legends, and the transcription reactions were allowed to proceed for 30 (for U6) or 90 (for Ad2 ML) min at 30°C.

15. A. Lesquire *et al.*, *EMBO J.* **13**, 1166 (1994).  
 16. T. Tamura *et al.*, *Nucleic Acids Res.* **19**, 3861 (1991).  
 17. S. Hashimoto, H. Fujita, S. Hasegawa, R. Roeder, M. Horikoshi, *ibid.* **20**, 3788 (1992).

18. A. Hoffmann *et al.*, *Nature* **346**, 387 (1990); C. C. Kao *et al.*, *Science* **248**, 1646 (1990); M. G. Peterson, N. Tanese, B. F. Pugh, R. Tjian, *ibid.*, p. 1625.  
 19. E. Noguchi *et al.*, GenBank accession number D30051.  
 20. K. Nakashima *et al.*, *Gene* **152**, 209 (1995).  
 21. J. M. Hancock, *Nucleic Acids Res.* **21**, 2823 (1993); G. Imbert, Y. Trotter, J. Beckman, J. L. Mandel, *Genomics* **21**, 667 (1994).  
 22. S. M. Lobo and N. Hernandez, *Cell* **58**, 55 (1989).

23. We thank B. Ma for technical help; C. Sadowski, who initiated this project, for discussions and reagents; T. Kuhlman for help with the Ad2 ML in vitro transcriptions; W. Herr, B. Stillman, and W. Tansey for discussion and comments on the manuscript; and J. Duffy, M. Ockler, and P. Renna for artwork and photography. Funded in part by NIH grant R01GM38810.

22 August 1996; accepted 9 December 1996

## Structural Convergence in the Active Sites of a Family of Catalytic Antibodies

Jean-Baptiste Charbonnier,\* Béatrice Golinelli-Pimpaneau, Benoît Gigant, Dan S. Tawfik,† Rachel Chap, Daniel G. Schindler, Se-Ho Kim, Bernard S. Green‡, Zelig Eshhar, Marcel Knossow‡

The x-ray structures of three esterase-like catalytic antibodies identified by screening for catalytic activity the entire hybridoma repertoire, elicited in response to a phosphonate transition state analog (TSA) hapten, were analyzed. The high resolution structures account for catalysis by transition state stabilization, and in all three antibodies a tyrosine residue participates in the oxyanion hole. Despite significant conformational differences in their combining sites, the three antibodies, which are the most efficient among those elicited, achieve catalysis in essentially the same mode, suggesting that evolution for binding to a single TSA followed by screening for catalysis lead to antibodies with structural convergence.

Convergent evolution is a frequent outcome of the process of natural selection. At present, we know very little about this process, particularly with respect to proteins and their function. Among the unanswered questions are concerns about how many different ways a protein pocket can effect a given chemical transformation, and what elementary processes once existed and have then been discarded along the evolutionary pathway to the efficient enzymes we see today. Catalytic antibodies that are induced experimentally in real time offer a way to reveal much about enzyme evolution including questions about convergence (1). The proposal that antibodies with catalytic activity (abzymes) could be generated to an analog of a transition state (TSA) of the reaction to be catalyzed (2) has proved widely applicable (3). Now, instead of reporting a singular event via a structure we report and compare

J.-B. Charbonnier, B. Gigant, B. Golinelli-Pimpaneau, M. Knossow, Laboratoire d'Enzymologie et de Biochimie Structurales, CNRS, 91198 Gif sur Yvette Cedex, France. D. S. Tawfik, R. Chap, D. G. Schindler, S.-H. Kim, Z. Eshhar, Department of Chemical Immunology, Weizmann Institute, Rehovot 76100, Israel. B. S. Green, Department of Pharmaceutical Chemistry, Faculty of Medicine, Hebrew University, Jerusalem 91120, Israel.

\*Present address: DIEP, CEA, 91191 Gif sur Yvette, France.

†Present address: Centre for Protein Engineering, MRC Centre, Hills Road, Cambridge CB2 2QH, UK.

‡To whom correspondence should be addressed.

the best solutions to catalysis in a family of antibodies, thereby offering insight into the power of selection, through a screening for catalytic activity, even when it is only allowed to operate once.

Most abzymes have been identified by screening the immune response for binding to the hapten and then testing the best scoring clones for catalytic activity. X-ray structures of abzymes generated following this general protocol have begun to define relationships between the hapten used to elicit catalytic antibodies and the residues of these antibodies which effect catalysis

(4–8). With a more facile procedure, cat-ELISA, in which product-specific antibodies are used to detect the appearance of product after immobilized substrate is exposed to the supernatant of culture hybridoma cells, we were able to probe the entire hybridoma repertoire for catalytic antibodies (9). The catalytic antibodies D2.3, D2.4, and D2.5 were obtained by immunizing BALB/c mice with phosphonate 1, an analog of the oxyanion intermediate in the hydrolysis of 2, coupled to keyhole limpet hemocyanin (KLH) (Fig. 1), and identified with the use of catELISA. Among a total of 1570 hybrid clones derived from a single mouse, nine scored positive in this assay, a figure to be compared to 970 hapten-binding clones (9). Catalytic antibodies D2.3, D2.4, and D2.5 show specific and efficient hydrolysis, accelerated by up to five orders of magnitude, toward the *p*-nitrobenzyl ester 2 (Table 1) and are significantly more active than the other six catalytic clones that were identified (as determined by cat-ELISA).

The sequences of the variable domains of D2.3, D2.4, and D2.5 have been determined. The most extensive differences are found in the H3 loop (10 residues), which in D2.4 differs from those in D2.3 and D2.5 at four positions and by an insertion (10). Otherwise, the sequences present a high degree of identity, similar to that observed in families of catalytic antibodies elicited with the same hapten (11–13), as opposed to the extensive differences between se-

**Table 1.** Kinetic and structural data on antibodies D2.3, D2.4, and D2.5.

	D2.3	D2.4	D2.5
$k_{cat}$ (min <sup>-1</sup> )*	3.6	1.0	0.07
$K_m$ (μM)	280	300	340
$K_D^S/K_D^T$ TSA	$1.1 \times 10^5$	$3.3 \times 10^4$	$1.3 \times 10^3$
$k_{cat}/k_{uncat}^\dagger$	$1.3 \times 10^5$	$3.6 \times 10^4$	$2.5 \times 10^3$
Resolution (Å)	1.9	3.1	2.2
Precision of atomic positions‡ (Å)	0.25	0.35	0.25
Interactions of TSA 1 with the Fab			
Buried surface§ (Å <sup>2</sup> )	515	510	505
van der Waals contacts (nb)	86	96	76
Hydrogen bonds (nb)	5	5	5

\*The catalytic activity (per site) and binding parameters were measured as described (9, 19). Data for the most efficient of these antibodies, D2.3, have been reported (9); those for D2.4 and D2.5 are reported in a kinetic study of all three antibodies (19, 28). † $k_{uncat}$  is measured in the same buffer as used for measuring catalysis, the kinetic constant being extrapolated to zero buffer concentration, at constant ionic strength. ‡The precision of atomic positions is evaluated from the variation of the *R* factor with the resolution, according to the method of Luzzati (20). §An equivalent surface area is buried on the Fab side.

quences of hapten binding clones (12). In the structures of these Fabs complexed with the TSA 1, the framework regions of the three Fvs superpose exactly within experimental error [root-mean-square deviation (rmsd) = 0.35 Å over 111 C $\alpha$ ]. Features common to the three structures are described with the use of data for D2.3 (14), which extend to the highest resolution (1.9 Å). In D2.3, the overall orientation of the aryl phosphonate part of the hapten with respect to the Fab is similar to those reported for three other abzyme structures (5–7). In the complex, 90% of the accessible surface of TSA 1 is buried. The *p*-nitrobenzyl moiety of the TSA is buried in a hydrophobic cavity that was found to be conserved in antibodies to small aryl phosphonate haptens (6, 15) (Fig. 2A). The two negatively charged oxygens of the phosphonate make three hydrogen bonds with Fab residues. The *N*-glutarylglucinate part of the ligand makes two additional hydrogen bonds with residues of the L3 complementarity determining region (CDR). The extensive interactions of 1 with residues of the Fab account for the high affinity of Fab D2.3 for TSA 1 (Table 1).

The three abzymes have a hydrolytic activity with an acceleration that is correlated to their higher affinity for the TSA relative to the substrate (Table 1). Such a correlation is found for most abzymes (16, 17) and, in the case of hydrolysis, suggests that catalysis occurs mainly by stabilization of the rate-determining transition state,

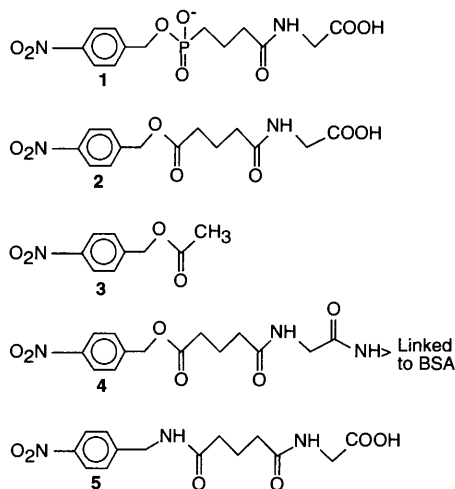


**Fig. 1.** Compounds used in this study. The structures of the antibodies are complexes with the hapten 1, which is the TSA used to elicit the three catalytic antibodies and for affinity measurements. Steady-state kinetics have been measured with substrate 2 (*p*-nitrobenzyl *N*-glutarylglucinate) and short substrate 3 (*p*-nitrobenzyl acetate). Catalytic antibodies were selected by cat ELISA with the substrate *p*-nitrobenzyl ester 4 (9). *p*-Nitrobenzyl amide glutaryl glucinate (5) is a substrate analog.

which is structurally similar to the negatively charged oxyanion intermediate. The contribution to catalysis of the differential stabilization of the TS (as reflected in binding to the TSA hapten) relative to substrate is best analyzed by considering successively three parts in these molecules, the reaction center (the neutral carbonyl in the substrate or the tetrahedral phosphonate in the transition-state analog) and the two flanking groups (the *p*-nitrobenzyl group and the *N*-glutarylglucinate). The *p*-nitrobenzyl part of the TSA makes tight interactions with 12 residues of the combining site that superpose well in the structures of D2.3 Fab complexed with TSA and of D2.3 Fab alone (rmsd: 0.24 Å); this suggests that Fab interactions with this part of the bound molecule are conserved in the substrate and in the transition-state analog. The two hydro-

gen bonds made between the *N*-glutarylglucinate part of the TSA 1 and the Fab account for 2 being a better substrate than *p*-nitrobenzyl acetate 3 for these antibodies (9).

In the combining site of D2.3, one phosphoryl oxygen of 1 is within the distance and angle for hydrogen bonding with two Fab residues (Tyr<sup>H100d</sup> and Asn<sup>L34</sup>), while the other P-O is similarly oriented with respect to Trp<sup>H95</sup> and a water molecule; this water molecule is not within hydrogen bonding distance of Fab residues (Fig. 2A). The interactions of the Fab with the first oxygen involve two hydrogen bond donors of the Fab. We therefore propose that Tyr<sup>H100d</sup> and Asn<sup>L34</sup> constitute the oxyanion hole in D2.3. Identical residues stabilizing the oxyanion are found in D2.4 (Fig. 2B) and this assignment is also consistent

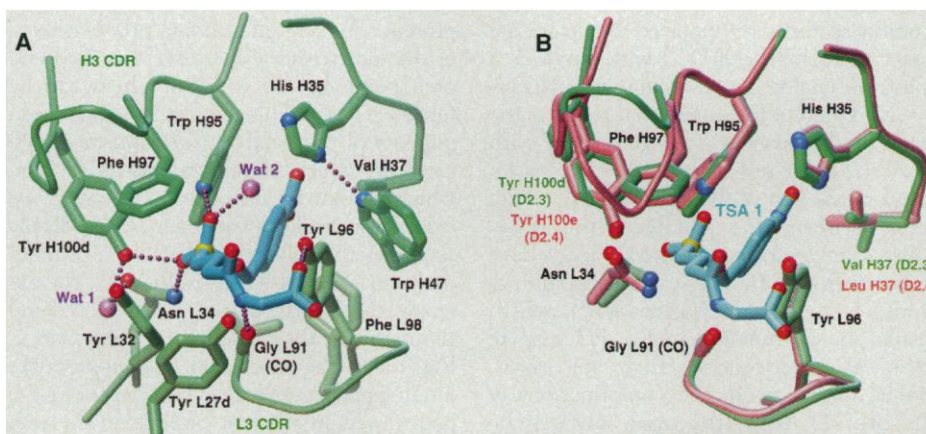
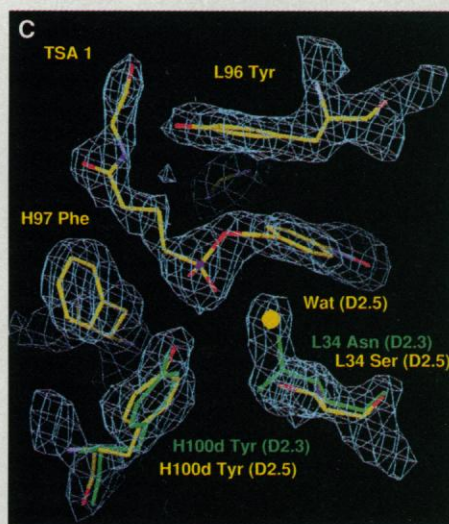


**Fig. 2.** (A) Schematic view of D2.3 Fab residues which contact the TSA 1 hapten, in blue. The C $\alpha$  trace of the Fab is in green and two water molecules are in pink. Hydrogen bonds are shown as dotted lines. Residue numbering is according to (21). Residues Tyr<sup>H100d</sup> and Asn<sup>L34</sup> constitute the oxyanion hole. Residues Val<sup>H37</sup>, Trp<sup>H47</sup> and Phe<sup>L98</sup> participate to the hydrophobic pocket surrounding the *p*-nitrobenzyl group [Figure rendered in the AVS environment (22)]. (B) Superposition of D2.3 and D2.4 combining sites (rmsd = 0.9 Å over 223 C $\alpha$  of variable regions). The oxyanion hole in D2.4 is provided by residues Tyr<sup>H100e</sup> and Asn<sup>L34</sup>. The interactions of D2.3 (green) and D2.4 (pink) H3 CDR with TSA 1 (blue) involve three residues (Trp<sup>H95</sup>, Phe<sup>H97</sup>, and Tyr<sup>H100d</sup> in D2.3 (H<sup>100e</sup> in D2.4)). The deviations of the C $\alpha$  positions of the three residues that contact the TSA (rmsd = 0.5 Å) are much smaller than the deviation of C $\alpha$ s over the whole H3CDR. The sequences of the H3 CDR are: D2.3 (H95 to H100d) WGF<sup>L</sup>EVRE<sup>D</sup>Y; D2.4 (H99 to H100e) WGFT<sup>L</sup>IVRE<sup>N</sup>Y. Underlined residues differ in the two sequences; the insertion is highlighted (figure rendered in the AVS environment). (C) 2F<sub>o</sub> - F<sub>c</sub> electron density map (at 2.2 Å resolution) in the combining site of D2.5 complexed with TSA 1. The map is contoured at 1.5  $\sigma$ . The frameworks of D2.5 variable domains have been superimposed on those of D2.3 (rmsd = 0.6 Å over 230 C $\alpha$ ). A water molecule (yellow), coordinated to Ser<sup>L34</sup>, is clearly visible in the electron density of D2.5 near the location of Asn<sup>L34</sup> N $\delta$ 2 in D2.3 (side chain, green). This water molecule is within hydrogen bonding distance to one of the phosphoryl oxygens of the TSA. Tyr<sup>H100d</sup> residues, which participate to the oxyanion hole, superpose well in both structures.



with structural data on D2.5. None of the amino acid changes between D2.3 and D2.5 affects TSA binding, except that of L34 (Asn → Ser), which involves one of the residues of the putative oxyanion hole. In the structures, the phosphonate and the main chain atoms of the Asn<sup>L34</sup> residue in D2.3 and of the corresponding Ser in D2.5 superpose very well (rmsd: 0.33 Å) (Fig. 2C). The hydroxyl of Ser<sup>L34</sup> in D2.5 is too far from the phosphonate for direct hydrogen bonding, and phosphonate stabilization involves a water molecule which is well defined in the electron density (Fig. 2C). In the three structures all other functional residues of the combining site that can promote nucleophilic or general base catalysis are further than 5 Å from the reaction center, which suggests that oxyanion stabilization plays a major role in catalysis in these antibodies.

The role of Tyr<sup>H100d</sup> in oxyanion stabilization is further supported by structural data on a complex of D2.3 with amide 5, a substrate analog: in this complex the carbonyl oxygen of the amide that replaces the ester of 2 makes a hydrogen bond with Tyr<sup>H100d</sup> (data not shown). Tyr<sup>H100d</sup> is located in the part of the structure that varies most between D2.3 and D2.4; this is because in these antibodies the H3 loops have matured from different joining recombinations of the D and J genes (10), which results in an insertion in the H3 loop of D2.4. As a consequence, there are considerable differences in the conformations of the two H3 loops (the rmsd between the C $\alpha$  positions is 2.0 Å over 10 C $\alpha$  atoms). Surprisingly, despite the structural differences, the hydrogen bonds between the TSA phosphonate and H3 are nearly identical in D2.3 and D2.4 (Fig. 2B).

The three most efficient abzymes identified among the repertoire elicited against a single TSA hapten display significant structural differences in their combining sites due both to a single amino acid change and to an insertion in the H3 loop. Both changes directly affect residues in contact with 1 and occur in addition to mutations remote from the combining site, as found in the study of affinity maturation of another catalytic antibody with esterase activity (7). Despite these changes, the three antibodies bind the hapten in essentially the same mode. Also, the same catalytic solution that was implicit in the design of a phosphonate TSA, stabilization of the oxyanion intermediate, has apparently been used by these

three antibodies. The diversity of the catalytic binding modes of the most efficient abzymes elicited in response to 1 is therefore more reduced than the diversity of binding antibodies that has been suggested by previous studies (12, 18); this may reflect the stringent constraints imposed by the precise positioning of the antibody combining site binding groups required to give rise to catalysis.

In our study, where the antibodies have been selected for catalysis from a pool that had evolved for binding, we witness structural convergence; despite significant structural differences in the combining site, the conformations of catalytic residues are similar. Although other hypotheses cannot be excluded this suggests that, reminiscent of what has been observed in enzymes, the combining sites of these antibodies result from convergent evolution, albeit in real time and involving a limited portion of the protein. The central question now is whether the mechanism we observe is a dead end or a point on the pathway which can be further refined. This reduces to which components of the catalytic mechanism should be kept, which should be discarded, and which could be modified. Certainly we would want to keep the features that deeply sequester the substrate and favor a tetrahedral and charged adduct. However, for example, the way the oxyanion is stabilized and the nature of the nucleophile could change. Regardless, the generation of an appropriate binding pocket appears to be a step along the pathway to an efficient catalyst. In the end, the described catalytic mechanism is functional and thus, through alternate cycles of mutagenesis and selection, it seems possible to make it evolve further.

## REFERENCES AND NOTES

- R. A. Lerner and K. D. Janda, in *Interface Between Chemistry and Biology*, P. Jolles and H. Jornwall, Eds. (Birkhauser, Basel, 1995).
- W. P. Jencks, *Catalysis in Chemistry and Enzymology* (McGraw-Hill, New York, 1969).
- R. A. Lerner, S. J. Benkovic, P. G. Schultz, *Science* **252**, 659 (1991).
- M. R. Haynes, E. A. Stura, D. Hilvert, I. A. Wilson, *ibid.* **263**, 646 (1994).
- G. W. Zhou, J. Guo, W. Huang, R. J. Fletterick, T. S. Scanlan, *ibid.* **265**, 1059 (1994).
- J.-B. Charbonnier *et al.*, *Proc. Natl. Acad. Sci. U.S.A.* **92**, 11721 (1995).
- P. A. Patten *et al.*, *Science* **271**, 1086 (1996).
- L. C. Hsieh-Wilson, P. G. Schultz, R. C. Stevens, *Proc. Natl. Acad. Sci. U.S.A.* **93**, 5363 (1996).
- D. S. Tawfik, B. S. Green, R. Chap, M. Sela, Z. Eshhar, *ibid.* **90**, 373 (1993).
- The sequences of the variable domains of D2.4 (resp. D2.5) differ from that of D2.3 at 3 (resp. 4)

positions in the light chain and 14 (resp. 11) positions in the heavy chain. Most differences in the combining site occur between D2.3 and D2.4, in the H3 loop; these loops result from the maturation through somatic mutations of different joining recombinations of the SP2-6.7 and Jh4 minigenes.

- J. Guo, W. Huang, G. W. Zhou, R. J. Fletterick, T. S. Scanlan, *Proc. Natl. Acad. Sci. U.S.A.* **92**, 1694 (1995).
- H. Miyashita *et al.*, *ibid.* **91**, 6045 (1994).
- T. S. Angeles, *et al.*, *Biochemistry* **32**, 12128 (1993).
- Details of purification and crystallization available from the authors. All data were recorded with synchrotron radiation at LURE. The space group symmetry of the crystals of D2.3 Fab unliganded and complexed with TSA 1 is *P3<sub>1</sub>21*;  $a = b = 78.2$  Å,  $c = 158.9$  Å,  $\alpha = \beta = 90^\circ$ ,  $\gamma = 120^\circ$ . Data were processed with MOSFLM (23) and the structure of the D2.3 Fab (IgG 2a,  $\kappa$ ) was solved by molecular replacement with the program AMoRe (24); the models used were the Fv domain and the CL-CH1 dimer of CNJ206, taken separately. The atomic model was established alternating cycles of reconstruction with program O (25) and of refinement with X-PLOR (26). The crystallographic *R* factor for the D2.3-1 complex is 21.5% ( $R_{\text{free}} = 26.1\%$ ) for all data larger than two standard deviations with data in the 7 to 1.9 Å range. For the unliganded structure, the values are  $R = 20.2\%$  ( $R_{\text{free}} = 25.2\%$ ) in the 7 to 2.5 Å range. The space group symmetry of the crystals of D2.4 Fab complexed with TSA 1 is *C222*, with  $a = 99.3$  Å,  $b = 104.8$  Å,  $c = 223.8$  Å,  $\alpha = \beta = \gamma = 90^\circ$ ; the space group symmetry of the crystals of D2.5 Fab complexed with TSA 1 is *P2*, with  $a = 67.9$  Å,  $b = 76.9$  Å,  $c = 45.8$  Å,  $\alpha = \gamma = 90^\circ$ ,  $\beta = 94.7^\circ$ . D2.5 Fab (IgG 2a,  $\kappa$ ) and D2.4 Fab (IgG 1,  $\kappa$ ) structures were also solved by molecular replacement; models used were the D2.3 Fv in both cases, and the CL-CH1 dimer of D2.3 (D2.5 structure) or of 3D6 (D2.4 structure) (27). The same refinement protocol as for D2.3 was used for D2.5 and D2.4 and the final crystallographic statistics are, respectively,  $R = 20.4\%$  ( $R_{\text{free}} = 26\%$ ) for data in the 7 to 2.2 Å range and  $R = 19.8\%$  ( $R_{\text{free}} = 29\%$ ) for data in the 7 to 3.1 Å range. The stereochemistry of all three catalytic antibodies is within expected values, given the respective resolution of their diffraction data.
- G. MacBeath and D. Hilvert, *Chem. Biol.* **3**, 433 (1996).
- R. Zemel, D. G. Schindler, D. S. Tawfik, Z. Eshhar, B. S. Green, *Mol. Immunol.* **31**, 127 (1994).
- J. D. Stewart and S. J. Benkovic, *Nature* **375**, 388 (1995).
- P. M. Alzari *et al.*, *EMBO J.* **9**, 3807 (1990).
- D. S. Tawfik, thesis, Weizmann Institute of Science (1995).
- V. Luzzati, *Acta Crystallogr.* **5**, 802 (1952).
- E. Kabat, *Sequences of Proteins of Immunological Interest* (National Institutes of Health, Washington, DC, 1991).
- C. Upson, *IEEE Comput. Graph. Appl.* **9**, 30 (1989).
- A. G. W. Leslie, *CCP4 and ESF-EACMB News. Protein Crystallogr.* **26** (1992).
- J. Navaza, *Acta Crystallogr. A* **50**, 157 (1994).
- T. A. Jones, J.-Y. Zhou, S. W. Cowan, M. Kjeldgaard, *ibid.* **47**, 1110 (1991).
- A. T. Brünger, *X-PLOR (Version 3.1) Manual* (Yale University, New Haven, CT, 1992).
- X. M. He, F. Rüker, E. Casale, D. C. Carter, *Proc. Natl. Acad. Sci. U.S.A.* **89**, 7154 (1992).
- D. S. Tawfik *et al.*, *Eur. J. Biochem.*, in press.
- We thank J. Janin and D. Thomas for reading of the manuscript and R. A. Lerner for stimulating discussions; M. Pique for enthusiastic help in making the figures; R. Fourme and J.-P. Benoit for assistance during the use of the LURE Synchrotron. Supported in part by D.G.A. grant 94/128 (M.K.).

3 May 1996; accepted 4 October 1996